water

MDPI

Article

Probability Distributions for a Quantile Mapping Technique for a Bias Correction of Precipitation Data: A Case Study to Precipitation Data Under Climate Change

Jun-Haeng Heo [1], Hyunjun Ahn [1,*], Ju-Young Shin [2,*], Thomas Rodding Kjeldsen [3] and Changsam Jeong [4]

1 Civil and Environmental Engineers, Yonsei University, Seoul 03722, Korea
2 Applied Meteorology Research Division, National Institute of Meteorological Sciences, Seogwipo 63568, Korea
3 Department of Architecture and Civil Engineering, University of Bath, Bath BA2 7AY, UK
4 School of Civil and Environmental Engineering, Induk University, Seoul 01878, Korea
* Correspondence: kamjakang@yonsei.ac.kr (H.A.); hyjyshin@gmail.com (J.-Y.S.); Tel.: +82-2-393-1597 (H.A.); +82-64-780-6560 (J.-Y.S.)

Received: 5 June 2019; Accepted: 11 July 2019; Published: 16 July 2019

check for updates

Abstract: The quantile mapping method is a bias correction method that leads to a good performance in terms of precipitation. Selecting an appropriate probability distribution model is essential for the successful implementation of quantile mapping. Probability distribution models with two shape parameters have proved that they are fit for precipitation modeling because of their flexibility. Hence, the application of a two-shape parameter distribution will improve the performance of the quantile mapping method in the bias correction of precipitation data. In this study, the applicability and appropriateness of two-shape parameter distribution models are examined in quantile mapping, for a bias correction of simulated precipitation data from a climate model under a climate change scenario. Additionally, the impacts of distribution selection on the frequency analysis of future extreme precipitation from climate are investigated. Generalized Lindley, Burr XII, and Kappa distributions are used, and their fits and appropriateness are compared to those of conventional distributions in a case study. Applications of two-shape parameter distributions do lead to better performances in reproducing the statistical characteristics of observed precipitation, compared to those of conventional distributions. The Kappa distribution is considered the best distribution model, as it can reproduce reliable spatial dependences of the quantile corresponding to a 100-year return period, unlike the gamma distribution.

Keywords: bias correction; quantile mapping; climate model; precipitation; frequency analysis

1. Introduction

Outputs of climate models and remote-sensing data are used for modeling the hydrological process. When these data sets are applied to an analysis using hydrological modeling, biases in these data sets should be corrected and reduced, particularly to the precipitation application [1,2]. Biases are systematic errors produced from the climate models and estimation algorithms used in remote sensing [3–5]. For example, a bias may appear because of various causes, such as imperfect model parameterization, inadequate reference data length and quality, and insufficient spatial resolution. Therefore, bias correction techniques have been developed to overcome these limitations.

Eden et al. [6] attempted to identify any sources of climate model error, and reported that precipitation data corrected by a statistical correction method can be a good predictor for the observed data set at a global scale. Teng et al. [7] assessed the performances of several bias correction methods for precipitation data, and evaluated their impact on a runoff model. They reported that the quantile mapping (QM) and two-state gamma distribution mapping methods provide good performance. The QM method shows better performance than a simpler bias correction for the mean and variation in the precipitation data [8–10]. Themeßl et al. [11] reported that QM leads to the best performance for precipitation, particularly to large amounts of quantiles. While the QM method provides a good performance for the bias correction of stationary data, it leads to less reliable results for nonstationary data, such as simulation data under a climate change scenario. To address this drawback, Cannon et al. [12] suggested the quantile delta mapping (QDM) method which explicitly preserves relative changes in all of the quantiles of the distribution. They claimed that the QDM method is superior to the traditional QM method and the detrended quantile mapping (DQM) method, which considers trends in the mean.

The QM method assumes that the distribution of simulated or estimated data preserves the distribution of any observed data. In QM, simulated data corresponding to a given probability is replaced by an observed quantile corresponding to the same probability. The probability distribution models of observed and simulated data are essential for QM. Hence, selecting an appropriate probability distribution model is critical for successfully implementing the QM method. Gamma distribution (GAM) has been widely used for the probability distribution of precipitation [13–15]. Because of its generality and simplicity, GAM is also commonly employed in the QM of precipitation.

Other probability distribution models, such as the exponential (EXP), Weibull, mixture of EXP, and mixture of GAM and Gumbel (GUM) distributions have been suggested for probability distributions of precipitation [16–18]. Many studies have reported that the fits of other distributions are preferred to those of GAM for the probability distribution of precipitation. Papalexiou and Koutsoyiannis [19] examined the potential of using maximum entropy with the Boltzmann–Gibbs–Shannon entropy definition for a probability distribution of rainfall worldwide. The generalized GAM and Burr Type XII (BUR) distributions performed very well. Ye et al. [20] examined distributional alternatives for the wet-day series of daily precipitation at point and catchment scales in the United States. Both the Pearson Type-III (P3) (also known as three-parameter GAM), and kappa (KAP) distributions performed very well, particularly for point rainfall. They claimed that KAP is the best distribution of wet-day precipitation at a point scale. The generalized GAM, BUR, and KAP distributions have two shape parameters. Because of their two-shape parameters, these distribution models can describe various distribution types. For instance, KAP can describe generalized extreme value (GEV), generalized pareto, and generalized logistics (GLO) distributions. The great flexibility of two-shape parameter distributions improves the fit of distribution for simulated and observed precipitation data in the QM method. This improvement can enhance the capacity of the QM method for correcting biases. Hence, two-shape parameter distributions should be employed in the QM method in simulating precipitation data.

The current study aims to investigate the fits and appropriateness of two-shape parameter distribution models in QM for the bias correction of precipitation data. For the investigation, we use simulated precipitation data from a climate model under a climate change scenario in South Korea. The employed distribution fits are assessed using the L-moment ratio diagram and Bayesian Information Criterion (BIC). Basic statistics and the Expert Team on Climate Change Detection, Monitoring and Indices (ETCCDI) are used as criteria for an evaluation of their appropriateness in the QM of employed precipitation data. Their fits and appropriateness are compared to those of the conventional distribution models. Additionally, a frequency analysis of the annual maximum precipitation from corrected precipitation data is conducted for assessing the impacts of the used distributions on hydrological applications. Results of the current study can improve the performance of the QM method for the bias correction of precipitation data. In addition, these can provide insight regarding the uncertainty produced by distribution selection in QM on the frequency analysis of extreme precipitation.

The main interest of climate change studies is to assess the future change in the variable of interest under the selected climate change scenario. Because precipitation is the variable of interest in this study, the impact of the distribution selection in the bias correction method on future precipitation should be investigated. In the current study, the impacts of distribution selection on extreme precipitation frequency analysis are investigated.

2. Materials and Methods

2.1. Quantile Mapping Based Bias Correction Method

Even if a climate model enhances the realism of simulated regional climatic characteristics, some significant biases probably remain, particularly regarding precipitation [21–23]. Therefore, the outputs of climate models such as global (GCM) and regional (RCM) climate models have to be corrected [24]. Performances and the applicability of various bias correction techniques have been explored for correcting bias in the output of a climate model [25,26]. Because of the different characteristics of meteorological variables, bias correction methods provide different performances depending upon the variables of interest [27,28]. In a bias correction of precipitation data, the quantile mapping (QM), the detrended quantile mapping (DQM), and the quantile delta mapping (QDM) methods have been widely employed because they can correct biases considering high order moment [12]. Additionally, these methods were designed to preserve long-term changes in quantiles projected by climate models [12,29]. Thus, the QM-based bias correction method is employed in this study.

QM corrects bias in the simulated data from an RCM by mapping quantiles at the same cumulative probability from the simulated data and the observed data sets. The equation of QM is as follows:

$$Q_m(t) = F_o{}^{-1}[F_s[Q_s(t)]] \tag{1}$$

where $Q_m(t)$ and $Q_s(t)$ are tth bias corrected data and simulated data from the RCM during the reference period (also known as the historical period), F_s and $F_o{}^{-1}$ are the cumulative distribution function (CDF) of the raw data from the RCM and the inverse CDF of the observed data, respectively.

It is impossible to obtain the probability distribution of the variable of interest for a future period. In the analysis of climate change projection, future simulation data is forced based on a climate change scenario. In QM, the probability distribution of the observed data for a future period is assumed to be the same. Because of the assumption of the same distribution of the observed data for the present and future periods, the long-term trend simulated by a climate model can be biased in QM. Cannon, Sobie, and Murdock [12] proposed the QDM method that is designed to correct the bias in climate projections, preserving the advantage of QM and the long-term trend in the output of the climate model. They reported that QDM minimized the GCM trend and bias, whereas QM possibly expands the climate change signals of any precipitation extremes simulated by the GCM. QDM is expressed as follows:

$$\delta_f(t) = \frac{Q_{s.f}(t)}{F_{s.r}{}^{-1}[F_{s.f}[Q_{s.f}(t)]]} \tag{2}$$

$$Q_m(t) = F_o{}^{-1}[F_{s.f}[Q_{s.f}(t)]] \times \delta_f(t) \tag{3}$$

where $\delta_f(t)$ and $Q_{s.f}(t)$ are a relative change in the tth quantiles between the reference and the simulation data and the tth quantile of simulated data during a predefined future period, respectively. $F_{s.f}$ and $F_{s.r}{}^{-1}$ are a CDF of the simulation data during a predefined future period, and an inverse CDF of the simulated data during the reference period, respectively.

A procedure of QDM can be divided into two steps in sequence: (1) Calculating the absolute or relative changes $\delta_c(t)$ in Equation (2) in the quantiles between the reference and future periods and (2) obtaining bias-corrected future projections $Q_m(t)$ in Equation (3) by multiplying the relative changes by the historical bias-corrected value. The algorithm composed of the two steps shows that not only can the bias in the data of the future projections period be corrected, but also the absolute or relative changes in quantiles can be conserved at the same time. More details regarding the concepts and algorithm of QDM can be found in Cannon, Sobie, and Murdock [12]. For the reference period, QDM is identical to QM because it is assumed that there is no change during the period. In the current study, QDM is employed as the bias correction method for the precipitation data.

2.2. Probability Distribution Models for Precipitation Data

The selecting of an appropriate probability distribution model is critical to successfully employing QDM in bias correction. Thus, these distribution model fits on the simulated and observed data sets should be evaluated, and their appropriateness should be assessed for bias. In this study, eight probability distribution models are tested for the candidate distribution in QDM.

2.2.1. Conventional Probability Distribution Models

The exponential (EXP) is used to model non-negative and positively-skewed data. The EXP has one scale parameter. Because of its simplicity, the EXP has been employed in many fields [30–32]. Because precipitation is non-negative and positively skewed data, the EXP has often been used for modeling the amount of a precipitation event [33,34]. The Gamma distribution method (GAM) has been widely used to model precipitation data [35–37]. In addition, GAM has often been employed in a QM-based method for a bias correction of simulated precipitation data [38,39]. GAM has two parameters: One scale and one shape parameter. Generalized extreme value (GEV) has been proposed for modeling extreme events [40,41]. The GEV has three parameters: One location, one scale, and one shape parameter. Gumbel (GUM) distribution is a sub-family of the GEV. When the shape parameter is equal to zero, the GEV distribution becomes GUM. The GEV and GUM have been broadly employed in extreme precipitation analysis [42–45].

2.2.2. Probability Distribution Models with a Two-Shape Parameter

Conventional distribution models have one or no shape parameter. Because precipitation data are largely affected by local characteristics such as terrain shape and geographical location, conventional distribution models sometimes result in a poor fit. Hence, a two-shape parameter probability distribution model can be an alternative for candidate distribution in modeling precipitation data, in which conventional distribution models provide an inadequate fit [46–48]. Generalized Lindley distribution (GLD) is an extension of a specific form of an EXP and GAM mixture distribution [49]. Hence, GLD can cover the EXP, GAM and Weibull distributions. Because the EXP and GAM distributions are often employed to model precipitation data, the GLD may show a good performance in modeling precipitation data. The GLD has two shape parameters. Burr Type XII (BUR) and kappa (KAP) distributions have been employed for modeling heterogeneous data [50–52]. BUR has three parameters: One scale and two shape parameters. The KAP distribution has four parameters: One location, one scale, and two shape parameters. Because these distribution models have two shape parameters, they have several sub-family distributions. For example, generalized pareto, generalized logistic and exponential distributions are a special form of KAP. CDF forms of the eight employed distributions are presented in Table 1.

Note that $\Gamma()$ and $\gamma(\,)$ are a gamma function and a lower incomplete gamma function, respectably.

Table 1. The employed probability distribution models.

Model	Cumulative Distribution Function
Gumbel	$F(x;\mu,\alpha) = \exp\left\{-\exp\left[-\frac{(x-\mu)}{\alpha}\right]\right\}$
Generalized extreme value	$F(x;\mu,\alpha,\beta) = \exp\left[-\left(1-\frac{\beta(x-\mu)}{\alpha}\right)^{(1/\beta)}\right]$
Gamma	$F(x;\alpha,\beta) = \frac{\gamma\left(k,\frac{x}{\alpha}\right)}{\Gamma(\beta)}$
Exponential	$F(x;\lambda) = 1-e^{-\lambda x}$
Kappa	$F(x;\mu,\alpha,\beta,h) = \left[1-h\{1-\beta(x-\mu)/\alpha\}^{1/\beta}\right]^{1/h}$
Burr XII	$F(x;\alpha,c,k) = 1-\frac{1}{\left(1+\left(\frac{x}{\alpha}\right)^{c}\right)^{k}}$
Generalized Lindley	$F(x;\lambda,\alpha) = \left[1-\frac{1+\lambda+\lambda x}{1+\lambda}\exp(-\lambda x)\right]^{\alpha}$

2.3. Case Study of Simulation Data Under a Climate Change Scenario in South Korea

2.3.1. Simulation Data for Climate Change Scenarios

For the projection of future climate change, GCMs have been commonly used because these models do not require boundary conditions in a continuous simulation. However, GCMs have limitations in resolution for showing the effect of local-to-regional-scale forcings (e.g., complex terrain, indented coastline and East Asia's monsoonal climate) [53–55]. Because of these limitations, the Intergovernmental Panel on Climate Change (IPCC) also advises research regarding climate change assessment and projection in which RCM outputs are used as reference climate scenarios [56,57]. To overcome these limitations, through additional study and various international collaborative research, RCMs that include more detailed information at spatial and temporal scales have been provided, such as the those of the North American Regional Climate Change Assessment Program (NARCCAP), Modelling the Impact of Climate Extremes (MICE), and the COordinated Regional Downscaling EXperiment (CORDEX) [58–62].

In South Korea, various RCMs, driven by Atmosphere-Ocean-coupled Hadley center Global Environmental Model version 2 (HadGEM2-AO) (Met Office, Exeter, UK.), have been performed through the CORDEX-East Asia (EA) projects and the participation of the Fifth Assessment Report (AR5) of the IPCC. The National Institute of Meteorological Sciences produced simulation data of the Hadley Centre Global Environmental Model Version 3-Regional Atmosphere (HadGEM3-RA) with 12.5-km resolution under the AR5 scenario as a national standard climate change scenario. More detailed descriptions of simulated data using HadGEM2-AO and HadGEM3-RA can be found in the Global Atmosphere Watch of the Korea Meteorological Administration (KMA) at www.climage.go.kr; the simulation data can be downloaded from cordex-ea.climate.go.kr.

In this study, daily precipitation of future climate simulated by HadGEM3-RA in COREDX-EA is projected based on the Representative Concentration Pathway (RCP) 4.5 scenario. The simulation data from HadGEM3-RA have been widely employed in climate studies for East Asia, including South Korea [63,64]. Kim et al. [65] reported that HadGEM3-RA can suitably simulate the statistical characteristics of extreme rainfall quantiles in South Korea. The domain of HadGEM3-RA includes Korea and some parts of China and Japan. HadGEM3-RA has 200 (west–east) × 180 (north–south) grid points. The reference period of model is from 1979 to 2005 and the future scenario is from 2011 to 2100.

2.3.2. Observed Data

In this study, 60 weather stations equipped with an Automated Synoptic Observing System (ASOS) network and managed by the KMA are selected. The stations are spread across South Korea, and the spatial resolution of inter-station spacing is approximately 1670 km^2. Figure 1 and Table 2 show the geophysical location and information of the stations employed in this study. The meteorological data set was recorded from 1961 to 2017, and the recording lengths of each station differ. Thus, to synchronize the recording period of the simulation data from the RCM, a daily precipitation data set observed from 1979 to 2005 is employed for bias correction in this study.

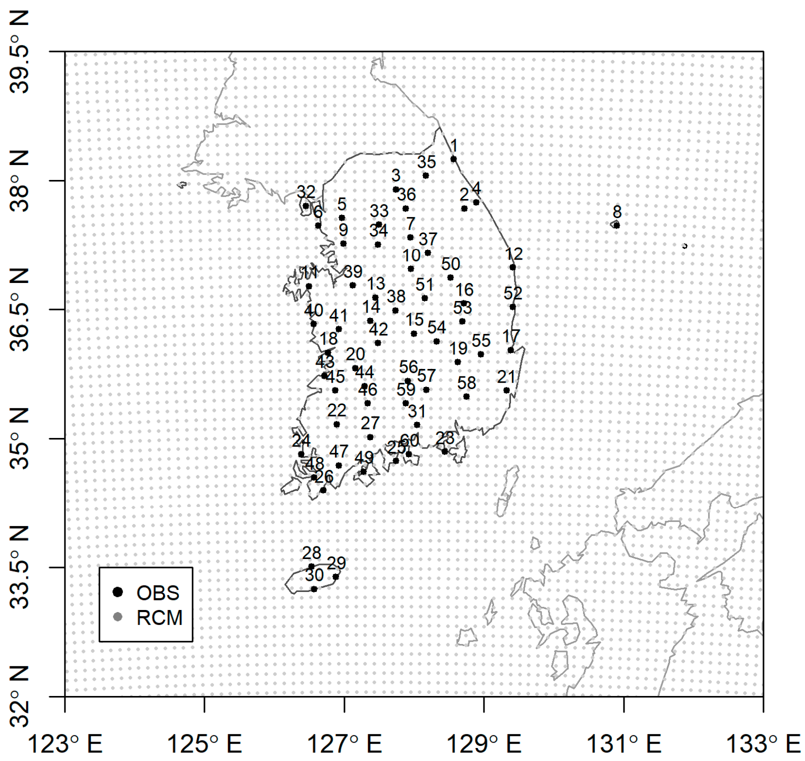

Figure 1. Locations of employed weather stations and the grid points of simulated data.

Table 2. Information of the used stations.

No.	Name	Latitude	Longitude	No.	Name	Latitude	Longitude
1	Daegwallyeong	128.72	37.68	31	Yeongdeok	129.41	36.53
2	Jecheon	128.19	37.16	32	Pohang	129.38	36.03
3	Chungju	127.95	36.97	33	Namhae	127.93	34.82
4	Wonju	127.95	37.34	34	Tongyeong	128.44	34.85
5	Yangpyeong	127.49	37.49	35	Geumsan	127.48	36.11
6	Icheon	127.48	37.26	36	Chupungnyeong	127.99	36.22
7	Inje	128.17	38.06	37	Boeun	127.73	36.49
8	Chuncheon	127.74	37.90	38	Daejeon	127.37	36.37
9	Hongcheon	127.88	37.68	39	Cheongju	127.44	36.64
10	Seoul	126.97	37.57	40	Buyeo	126.92	36.27
11	Suwon	126.99	37.27	41	Cheonan	127.12	36.78
12	Incheon	126.63	37.48	42	Seosan	126.50	36.77
13	Ganghwa	126.45	37.71	43	Gunsan	126.76	36.00
14	Sokcho	128.57	38.25	44	Boryeong	126.56	36.33
15	Gangneung	128.89	37.75	45	Jeonju	127.16	35.82
16	Andong	128.71	36.57	46	Jeongeup	126.87	35.56
17	Yeongju	128.52	36.87	47	Buan	126.72	35.73
18	Mungyeong	128.15	36.63	48	Imsil	127.29	35.61
19	Uiseong	128.69	36.36	49	Namwon	127.33	35.41
20	Gumi	128.32	36.13	50	Wando	126.70	34.40
21	Daegu	128.62	35.89	51	Suncheon	127.37	35.02
22	Yeongcheon	128.95	35.98	52	Goheung	127.28	34.62
23	Geochang	127.91	35.67	53	Yoesu	127.74	34.74
24	Hapcheon	128.17	35.57	54	Gwangju	126.89	35.17
25	Sancheong	127.88	35.41	55	Jangheung	126.92	34.69
26	Jinju	128.04	35.16	56	Haenam	126.57	34.55
27	Miryang	128.74	35.49	57	Mokpo	126.38	34.82
28	Ulsan	129.32	35.56	58	Jeju	126.53	33.51
29	Ulleungdo	130.90	37.48	59	Seogwipo	126.57	33.25
30	Uljin	129.41	36.99	60	Seongsan	126.88	33.39

2.3.3. Case Study Methodology

To assess the applicability of probability distribution models using a two-shape parameter, any fits of the employed probability distribution models for the observed and simulated precipitation data, and the appropriateness of the probability distribution models for the bias correction of the precipitation data, are evaluated. The maximum likelihood method is used to fit EXP, GAM, GEV, GUM, BUR, and GLD [49,66,67]. KAP is fit using the L-moment method [68]. The distributional characteristics of the observed and simulated data are investigated using an L-moment ratio diagram. The L-moment ratio diagram has been broadly used to investigate the distributional characteristics of the data and the fits of this probability distribution [69,70].

BIC are employed for assessments of the fits of employed probability distributions. BIC is provided as follows:

$$BIC = -2LL + \log(n)k \tag{4}$$

where LL, n, and k are the log-likelihood, number of data and number of parameters, respectively. Because of the penalty term $\log(n)k$ for the number of parameters in the distribution model, this criterion considers parsimony. The numbers of the parameters in the two-shape parameter distribution models are larger than those of the conventional distribution models. BIC is a good evaluation measure of goodness-of-fit for the employed distribution models in the current study, particularly the distributions with two-shape parameters. As BIC decreases, the fit of the given distribution to the sample data increases. BIC is a more severe criterion than the Akaike information criterion in the current study, because the number of data points is greater than 2000.

The indices of the Expert Team on Climate Change Detection, Monitoring and Indices (ETCCDI), which are climate extremes indices, are employed in the current study. ETCCDI was proposed for representing the characteristics of extreme events of precipitation and temperature in the same manner, such that their analyses fit seamlessly into the global picture [71]. The ETCCDI indices are widely used to evaluate and describe model projections of the future using specific physically-based thresholds [29].

All used ETCCDI indices are described in Table 3. As shown in Table 3, mean, standard deviation, coefficient of skewness and PRCPTOT represent the data statistical characteristics. SDII, Rx1day, Rx5day, R95pTOT, and R95pTOT represent those characteristics of extreme precipitation events. Therefore, the appropriateness of the tested distribution models can be evaluated through a comparison of the ETCCDI indices for the observed and bias-corrected data.

Table 3. The indices used to represent characteristics of precipitation.

Acronym	Description	Unit
Mean	Mean daily precipitation	mm
SD	Standard deviation of daily precipitation	mm
CS	Coefficient of skewness of daily precipitation	-
PRCPTOT	Annual total precipitation in wet days (daily precipitation ≥ 1 mm)	mm
SDII	Annual precipitation divided by the number of wet days	mm/day
Rx1day	Annual maximum 1-day precipitation	mm
Rx5day	Annual maximum 5-day precipitation	mm
R95pTOT	Annual total rainfall when daily precipitation > 95 percentile	mm
R99pTOT	Annual total rainfall when daily precipitation > 99 percentile	mm

The annual maximum precipitations are extracted from the bias-corrected data. The future period is divided into three sub-periods: S1 (2011–2040), S2 (2041–2070), and S3 (2071–2100). Quantiles corresponding to a 100-year return period are calculated for all stations and the results of the quantile estimation are spatially distributed. GUM is used for the frequency analysis of extreme precipitation in this study because GUM was recommended by the government for modeling extreme precipitation in South Korea [72].

3. Results

To examine the statistical characteristic of data, L-moment ratio diagrams are employed. The L-moment ratio diagram is well known as a useful graphical method for investigating the distribution characteristics of data sets [73–75]. Figure 2 shows L-moment ratios for the observed data (OBS) of 60 stations in South Korea as red dots and the simulation data (REF) as black dots for the reference period. These data sets, with a few exceptions of REF, fall above the theoretical curve of P3 (shown in blue) and below both the theoretical curves of Generalized Pareto (GPA, shown in yellow) and Generalized Normal Distribution (GNO, shown in green). OBS and REF are included in the theoretical area of KAP, but not in the theoretical area of BUR. Some OBS and REF dots are distributed within a similar L-skewness and L-kurtosis range. However, the OBSs overall have a larger L-skewness and L-kurtosis than those of the REF. Although some stations in REF follow a P3 distribution (also known as a three-parameter GAM), many stations of REF may follow P3, GNO or GPA. For OBS, there is no dominant distribution model; they may also follow one of the P3, GNO and GPA models.

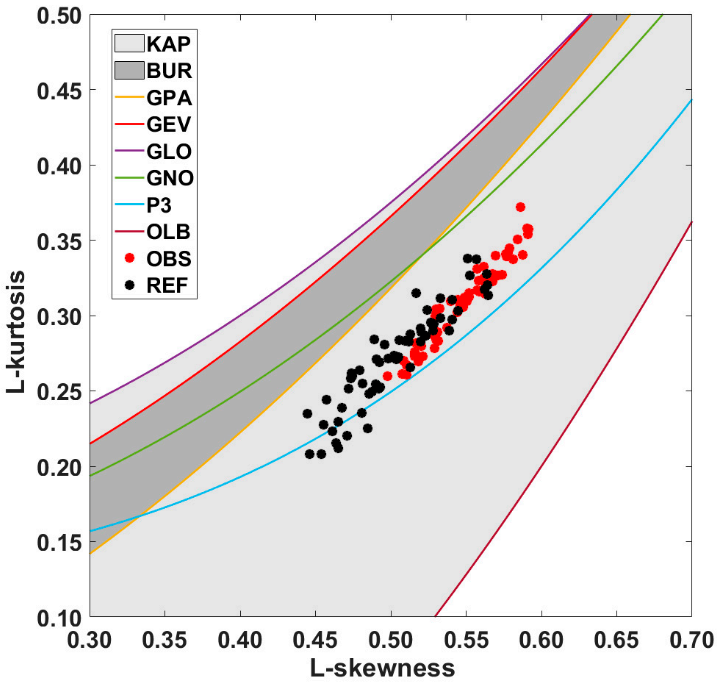

Figure 2. L-moment ratio diagram for observed and simulated precipitation data. REF indicates simulation data for the reference period.

Figure 3 presents BIC boxplots of employed distribution models for OBS and REF. The boxes display the interquartile range (IQR), and the whiskers extend to 1.5 × IQR. The horizontal red lines inside the boxes depict the median of the data. Data beyond the whiskers (1.5 × IQR) are indicated by a plus sign (+). The size of each box represents the variability of BIC for the 60 stations employed in this study. The pattern of these results is quite similar, as shown in Figure 3a,b. All BIC medians for REF are lower than those of OBS. The lowest value of BIC median is that of KAP, the second lowest is that of GEV, and the largest is that of GUM. The BIC results for all distributions show that KAP is the best fit for OBS and REF. Table 4 presents the numbers of the distributions providing the smallest BIC for OBS and REF. KAP is selected at all employed stations as the best distribution based on BIC. The second-best distributions are BUR and GEV for OBS and REF, respectively. The distributions that have greater than three parameters lead to a good fit based on BIC even if BIC has the penalty term for the number of parameters. Based on BIC, KAP leads to a better fit than the two-parameter distributions such as GAM, GUM and GLD. The fit of KAP for OBS and REF is superior to other distributions models for precipitation in South Korea.

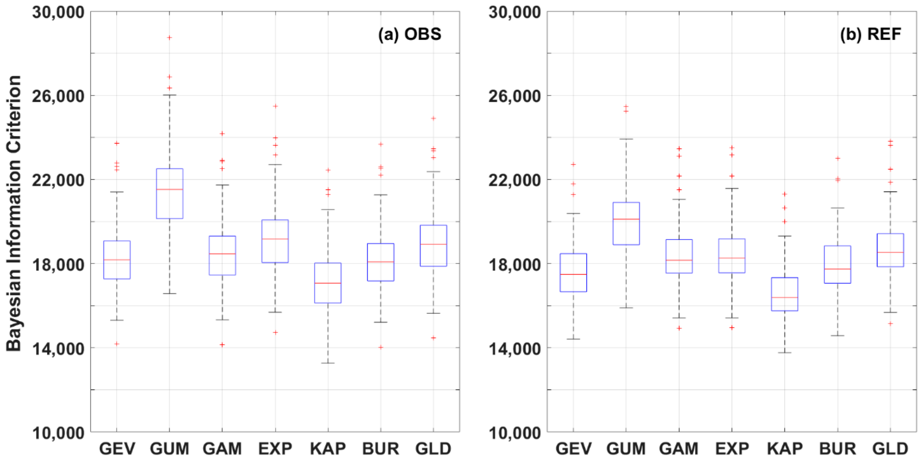

Figure 3. Boxplots of BIC for employed distribution models in the observed and simulated precipitation data periods.

Table 4. Results for the numbers of the distributions giving the smallest BIC among the employed probability distribution models for observed and simulated precipitation (reference period) data in South Korea.

Distributions	Observed Data			Simulated Data		
	1st	2nd	3rd	1st	2nd	3rd
GEV	-	9 (15%)	38 (63%)	-	60 (100%)	-
GUM	-	-	-	-	-	-
GAM	-	-	13 (22%)	-	-	1 (2%)
EXP	-	-	-	-	-	-
KAP	60 (100%)	-	-	60 (100%)	-	-
BUR	-	51 (85%)	9 (15%)	-	-	59 (98%)
GLD	-	-	-	-	-	-

Figure 4 presents basic statistics such as the mean, standard deviation (SD) and coefficient of skewness (CS) for the observed, simulated and bias-corrected data with the employed distributions. There are large differences between the basic statistics of OBS and REF. As shown in Figure 4a, the mean of KAP, EXP and GAM are similar to the mean of OBS. GEV and GLD are greater than OBS, and BUR is less than OBS. A shown in Figure 4b, the medians of the SDs of the bias-corrected data using KAP and GLD are close to the median of the SDs of OBS. GEV and BUR are different from OBS. Results for CSs are similar to the results for the SDs, but the presented CSs have a larger variability than those of the SDs. KAP leads to the best performance among the employed distributions for CSs. Because the CS can represent the behavior of extreme data, the bias-corrected data using KAP may show a good performance for extreme precipitation. Hence, KAP is the best distribution for reproducing the basic statistics of the observed data.

The PRCTOT and SDII indices among the ETCCDI indices are presented in Figure 5. For PRCPTOT, the boxes of GUM, GAM, EXP and KAP are similar to that of OBS. The distribution of PRCPTOT for KAP is the closest to that of OBS. The SDIIs of the bias-corrected data differ depending on the employed distribution models. Based on the SDII results, GAM and KAP provide good performance for bias correction. The distribution of SDII for KAP is more similar to that of the observed data than one of GAM. Rx1day, Rx5day, R995pTOT and R99pTOT for observed, simulated and bias-corrected data by employed distributions are shown in Figure 6. These indices represent the characteristics of extreme events in a given data set. The data bias-corrected using GUM, EXP and KAP provide a similar distribution to that of the observed data. GEV and BUR provide poor performances for reproducing extreme events. KAP leads to the best performance for the bias correction of precipitation based on the results of the ETCCDI indices.

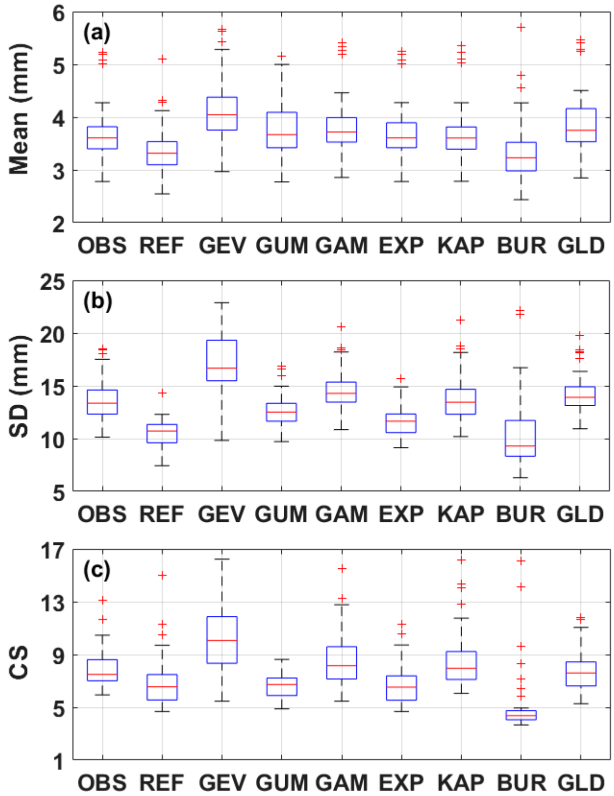

Figure 4. Boxplots of the basic statistics for employed distribution models in the observed and simulated precipitation data.

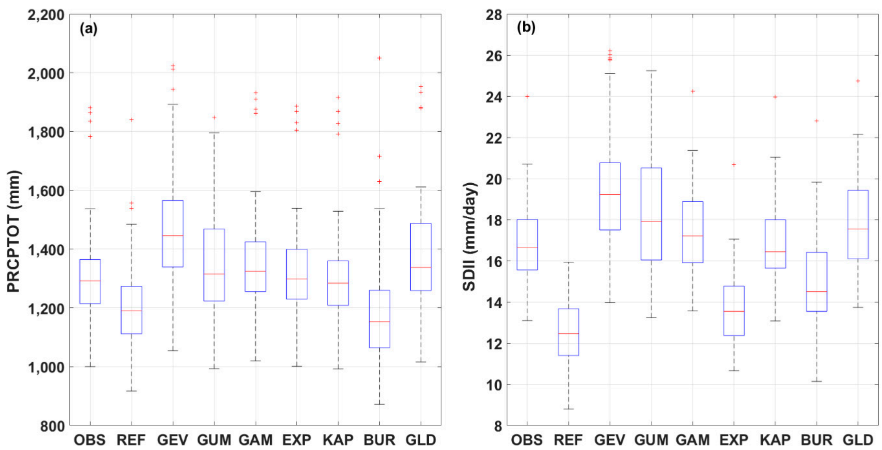

Figure 5. Boxplots of PRCTOT and SDII for employed distribution models in the observed and simulated precipitation data.

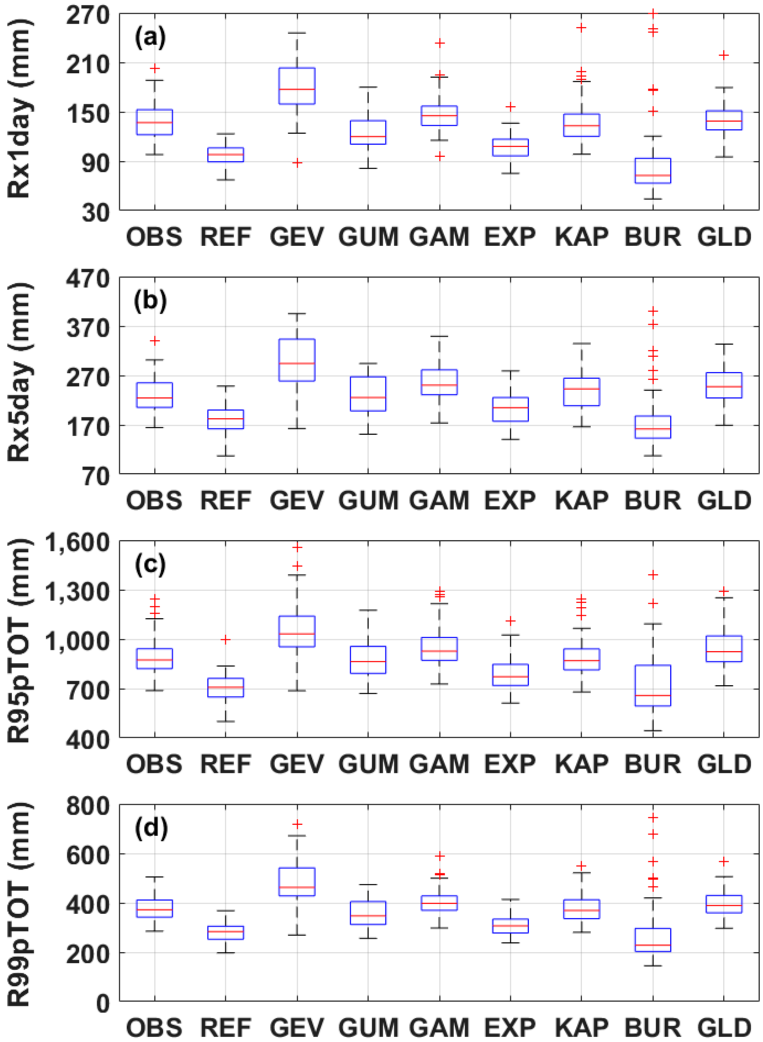

Figure 6. Boxplots of Rx1day, Rx5day, R95pTOT and R99pTOT for employed distribution models in the observed and simulated precipitation data.

Quantiles of OBS, REF and the bias-corrected data at six stations are shown in Figures 7 and 8. The quantiles are grouped into two parts: (1) Quantiles less than the 80th percentile and (2) quantiles equal to and greater than the 80th percentile to investigate correction performances on non-heavy and heavy precipitation events. Quantiles of OBS is bigger than quantiles of REF at the same non-exceedance probability, and the differences between the quantiles of OBS and REF increase when the non-exceedance probability increases. GEV, GAM and KAP lead to good performances for correcting bias in non-heavy precipitation events. For a bias correction of heavy precipitation, GAM and KAP show good performance. BUR does not work well in the bias correction of precipitation in South Korea. Overall, KAP leads to the best performance in the bias correction of precipitation.

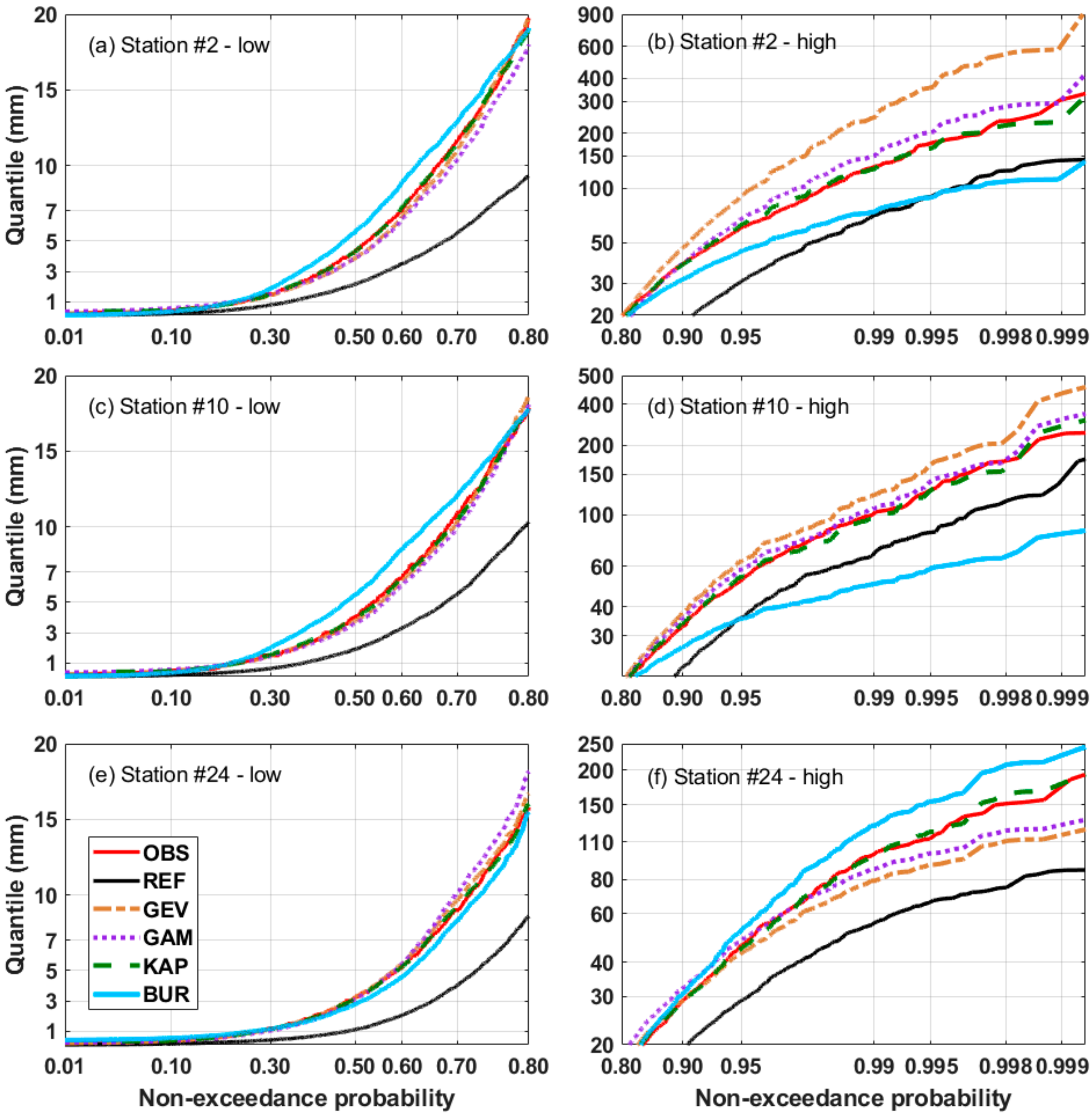

Figure 7. Quantile plots of generalized extreme value (GEV), Gamma distribution (GAM), kappa (KAP) distributions and Burr Type XII (BUR), and quantiles for the observed and simulated precipitation data at station #2, #10 and #24.

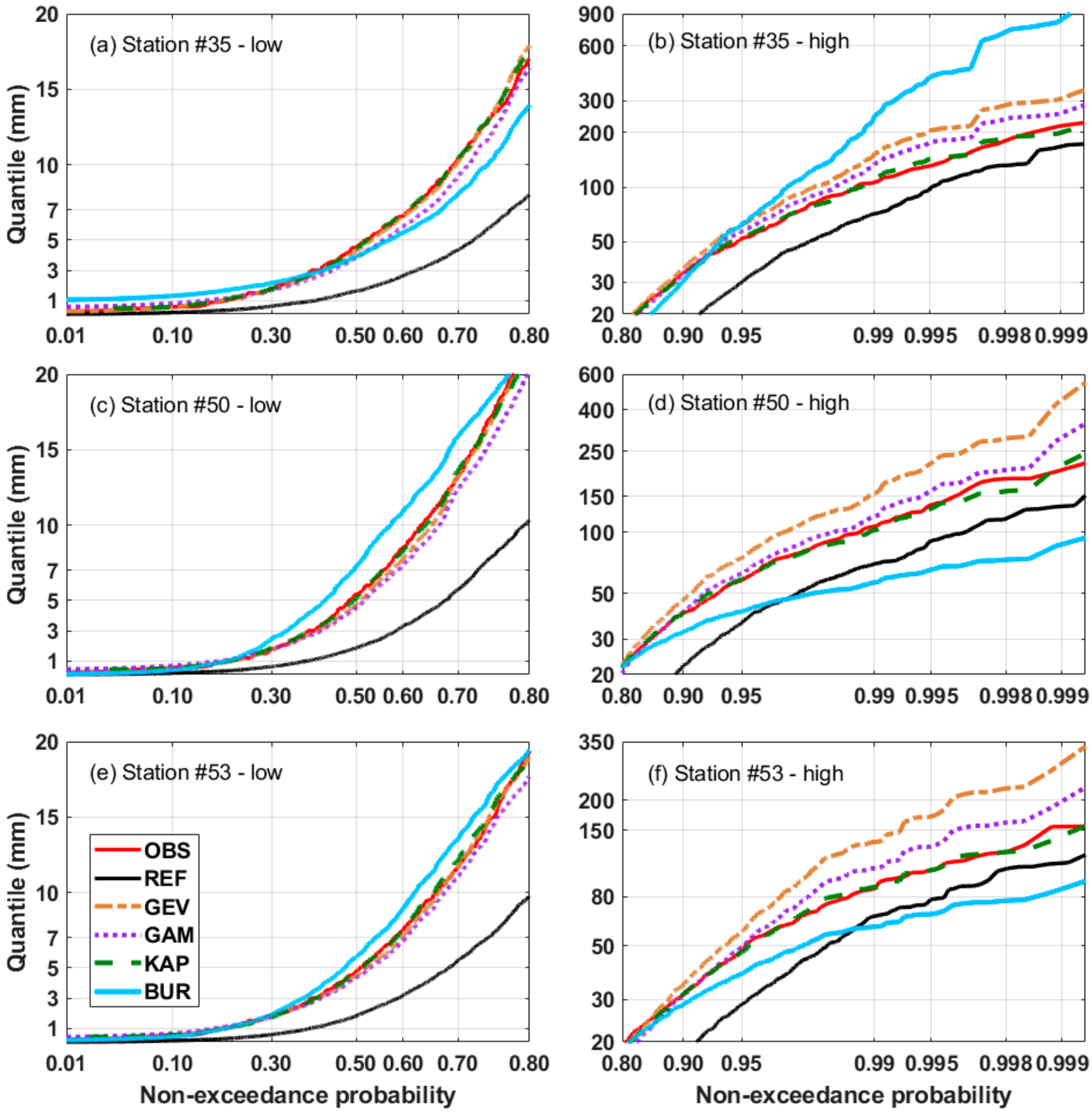

Figure 8. Quantile plots of GEV, GAM, KAP and BUR and quantiles for the observed and simulated precipitation data at station #35, #50 and #53.

Figure 9 presents a spatial distribution of quantiles corresponding to a 100-year return period for GAM and KAP. The quantiles from the two distributions increase over time. The quantiles from GAM are larger than those of KAP. Large differences are observed in the northeast and southwest regions. In the northeast region, GAM leads to much larger quantiles than those of KAP, while KAP leads to larger quantiles than those of GAM in the southwest region. To examine the detailed difference between GAM and KAP, the differences are shown spatially in Figure 10. The differences are calculated by subtracting the quantiles of GAM from the quantiles of the KAP. The aforementioned results are obviously shown in Figure 10. The difference patterns are similar for all periods. The ranges of the differences are from −150 to 200 mm. For most regions, the differences are very small (from −30 to 50 mm). GAM quantiles for some stations are much larger than the quantiles at the nearest station. These large differences are rarely observed in KAP quantiles. This result means that the application of KAP successfully preserves spatial dependence among stations while the application of GAM does not.

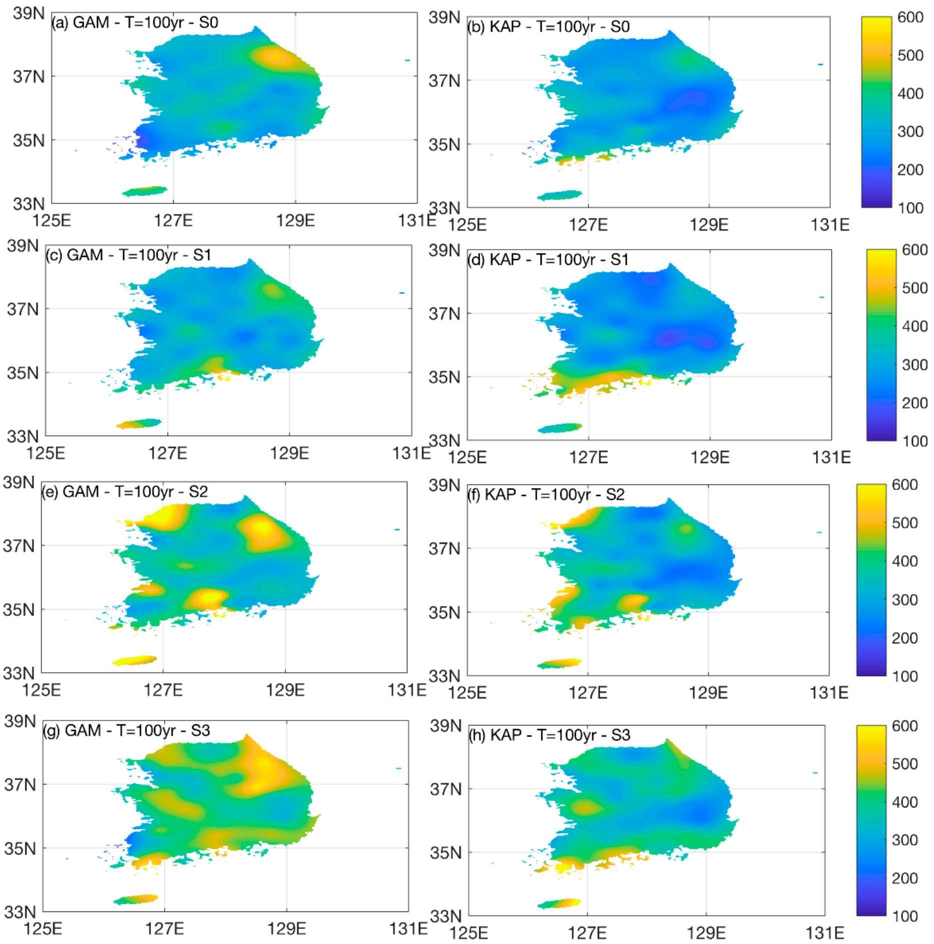

Figure 9. Spatial distributions of quantiles corresponding to a 100-year return period from GAM and KAP for reference and future periods.

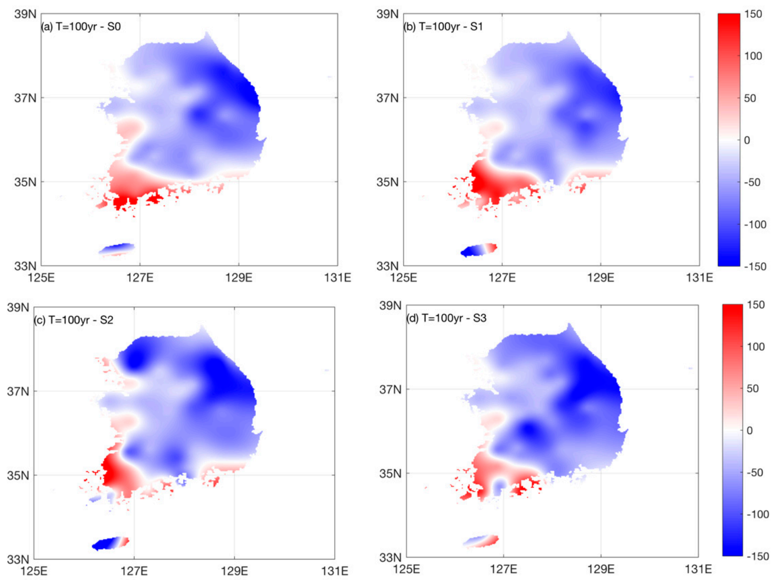

Figure 10. Spatial distributions of differences between quantiles of GAM and KAP corresponding to a 100-year return period for reference and future periods.

4. Discussion

In the current study, the applicability of two-shape parameter distribution is investigated for the bias correction of precipitation using QDM. As shown in Figure 2, the KAP can represent the statistical characteristics of all employed data, because all points (L-skewness and L-kurtosis) are inside of the area of KAP. The points also are near GPA, GNO and P3, but they may not successfully represent the statistical characteristics of the simulated precipitation data. Additionally, based on the results of the basic statistic and ETCCDI indices, GLD and KAP lead to good performances in reproducing the distributional characteristics of the observed precipitation data. The performance of KAP is superior to that of other employed distributions, and the performance of GLD is comparable to one of GAM. BUR provides a poor performance even if it is a two-shape parameter distribution. The two-shape parameter distributions have great flexibility because of their complexity. Thus, their performance should be assessed considering parsimony. KAP and BUR lead to a low BIC value, and the BIC of GLD is similar to the BICs of GAM and EXP. Even if complexity is considered in the assessment, their performances are better or comparable to the distributions that have one or no shape parameter. Hence, the two-shape parameter can be applied in QDM for a bias correction of precipitation, and they should be considered candidate distribution models for modeling precipitation in bias correction.

The most appropriate distribution model can be selected from the results for the bias correction of the precipitation data in South Korea. The best performances to reproduce the statistical characteristics of the observed precipitation are observed from KAP based on the results of the basic statistics and ETCCDI indices. Additionally, KAP has the largest number of parameters among the employed distribution models. Hence, BIC would be a severe evaluation measure for KAP because of the penalty term. KAP leads to the lowest BIC values among the employed distributions even if it receives the largest penalty. In Table 4, KAP is selected for all employed stations as the distribution providing the lowest BIC. In Figure 2, the points of OBS and REF are inside KAP. This result supports that KAP has a capacity to successfully represent the statistical characteristics of observed and simulated precipitation data in South Korea, unlike the other distributions. Therefore, KAP is the best distribution model among the employed distributions for QDM to bias-correct the simulated precipitation in South Korea. These results are consistent with the analysis results of the probability distribution for daily precipitation in the United States [20]. They report that KAP is the best distribution for modeling the daily precipitation on a wet day.

The main purpose of precipitation projection under climate change is to assess possible future change in phenomena related to precipitation, e.g., floods, droughts, drainage operation and crop yield prediction [76–79]. The current study focuses upon the impacts on the frequency analysis of extreme precipitation. As shown in Figures 9 and 10, there are large differences between the quantiles from GAM and KAP, even if their performances to reproduce statistical characteristics are similar. This result indicates that uncertainty from the distribution selection is large. Small differences in bias-corrected precipitation data can propagate to a large difference in analysis results for phenomena related to precipitation. For example, the maximum difference is 200 mm, and it is greater than 30% of the quantile. This difference can largely change the design criteria of hydraulic infrastructure such as dams and urban drainage systems.

GAM is often employed as a distribution model in bias correction of precipitation [12,80]. The appropriateness of GAM for modeling precipitation has been proved in an extensive body of literature [81–86]. As expected, GAM leads to good performance for reproducing the statistical characteristics of observed precipitation. However, GAM leads to poor performance for results of frequency analysis for extreme precipitation. As shown in Figure 9e, there are three yellow eyes (northwest, northeast, and south). These eyes indicate that the quantiles at these three locations are much larger than the quantiles of nearby locations. These eyes occur in a mountainous area and island because of geomorphological characteristics. Two of the eyes are on flat plains. Though quantiles at these two eyes can be different from the quantiles at nearby locations, the differences should be small.

This result supports that the quantiles from GAM inadequately reproduce the spatial dependence of extreme precipitation in South Korea.

Hence, KAP would be a better choice than GAM for the bias correction of precipitation simulated RCM in South Korea. Additionally, the appropriateness of these distribution models should be investigated through a simple case study to attenuate uncertainty from the bias correction method for the analyses of phenomena related to precipitation.

5. Conclusions

The current study aims to investigate the applicability and appropriateness of two-shape parameter distributions in QDM for a bias correction of precipitation simulated by an RCM. The applicability and appropriateness of seven distributions are evaluated and compared. Three of these are two-shape parameter distributions and the others have one or no shape parameter. An L-moment ratio diagram, BIC, basic statistics and ETCCDI are employed to assess their applicability and appropriateness through a case study of simulated daily precipitation data under the RCP4.5 climate change scenario in South Korea. In the current study, we reach the following conclusions:

1. Two-shape parameter distributions can be used in QDM for a bias correction of the daily precipitation data. The application of GLD and KAP distributions provide good performances in reproducing the statistical characteristics of observed precipitation data, while BUR leads to poor performance. KAP outperforms GAM, which is popularly used in QDM. Additionally, the performance of the GLD can be comparable to one of the GAM.
2. The KAP distribution is considered as the most appropriate distribution model in QDM for the bias correction of precipitation in South Korea. KAP gives the lowest BIC. Bias-corrected precipitation data using KAP successfully reproduces the basic statistics and extreme characteristics of the observed data. Particularly, KAP is superior to the other distributions for reproducing characteristics of extreme precipitation events.
3. Selection of an appropriate distribution model in QDM is very important in bias correction of precipitation data. The fit and appropriateness of GAM and KAP are better than that of the other employed distributions based on the results of basic statistics and ETCCDI indices. Results of frequency analysis for extreme precipitation bias-corrected using GAM and KAP present large differences. The precipitation bias-corrected using GAM seems to lose the spatial dependence of observed data during the S2 period, while precipitation data using KAP seems to preserve spatial dependences. When the precipitation data bias-corrected by the GAM are used for flood modeling considering climate change, the result can greatly influence the flood modeling results.

Although GAM would lead to a good performance in the bias correction of precipitation data based on the results of the evaluation measures, spatial dependences of quantiles from the frequency analysis of extreme precipitation using GAM is unrealistic. The influence of selecting a distribution model in QDM on modeling and analysis phenomena related to precipitation, such as flood and drought, remains questionable. To reduce uncertainty in the projection of a climate change scenario on modeling and analysis, the influences of selecting the distribution on the modeling and analysis of any phenomena related to precipitation should be investigated. In addition, simulated precipitation data in South Korea are employed to examine the applicability and appropriateness of two-shape parameter distributions in the current study. In other regions or countries, their applicability and appropriateness may be different. Thus, they are assessed in QDM for the bias correction of precipitation in other regions.

Author Contributions: Conceptualization, J.-H.H. and J.-Y.S.; methodology, H.A. and J.-Y.S.; software, H.A.; validation, J.-H.H., H.A. and J.-Y.S.; formal analysis, H.A. and J.-Y.S.; investigation, J.-H.H. and C.J.; writing—original draft preparation, H.A. and J.-Y.S.; writing—review and editing, T.R.K.; visualization, H.A. and J.-Y.S.; supervision, J.-H.H.; funding acquisition, C.J.

Funding: This work was supported by the National Research Foundation of Korea (NRF) grant funded by the Korea government (Ministry of Science, ICT & Future Planning) (No. 2017R1A2B4009338).

Conflicts of Interest: The authors declare no conflict of interest.

References

1. Hagemann, S.; Chen, C.; Haerter, J.O.; Heinke, J.; Gerten, D.; Piani, C. Impact of a Statistical Bias Correction on the Projected Hydrological Changes Obtained from Three GCMs and Two Hydrology Models. *J. Hydrometeorol.* **2011**, *12*, 556–578. [CrossRef]
2. Sillmann, J.; Kharin, V.V.; Zhang, X.; Zwiers, F.W.; Bronaugh, D. Climate extremes indices in the CMIP5 multimodel ensemble: Part 1. Model evaluation in the present climate. *J. Geophys. Res. Atmos.* **2013**, *118*, 1716–1733. [CrossRef]
3. Wilby, R.L.; Hay, L.E.; Gutowski, W.J., Jr.; Arritt, R.W.; Takle, E.S.; Pan, Z.; Leavesley, G.H.; Clark, M.P. Hydrological responses to dynamically and statistically downscaled climate model output. *Geophys. Res. Lett.* **2000**, *27*, 1199–1202. [CrossRef]
4. Wood, A.W.; Leung, L.R.; Sridhar, V.; Lettenmaier, D.P. Hydrologic Implications of Dynamical and Statistical Approaches to Downscaling Climate Model Outputs. *Clim. Chang.* **2004**, *62*, 189–216. [CrossRef]
5. Piani, C.; Weedon, G.P.; Best, M.; Gomes, S.M.; Viterbo, P.; Hagemann, S.; Haerter, J.O. Statistical bias correction of global simulated daily precipitation and temperature for the application of hydrological models. *J. Hydrol.* **2010**, *395*, 199–215. [CrossRef]
6. Eden, J.M.; Widmann, M.; Grawe, D.; Rast, S. Skill, Correction, and Downscaling of GCM-Simulated Precipitation. *J. Clim.* **2012**, *25*, 3970–3984. [CrossRef]
7. Teng, J.; Potter, N.J.; Chiew, F.H.S.; Zhang, L.; Wang, B.; Vaze, J.; Evans, J.P. How does bias correction of regional climate model precipitation affect modelled runoff? *Hydrol. Earth Syst. Sci.* **2015**, *19*, 711–728. [CrossRef]
8. Teutschbein, C.; Seibert, J. Bias correction of regional climate model simulations for hydrological climate-change impact studies: Review and evaluation of different methods. *J. Hydrol.* **2012**, *456*, 12–29. [CrossRef]
9. Gudmundsson, L.; Bremnes, J.B.; Haugen, J.E.; Engen-Skaugen, T. Technical Note: Downscaling RCM precipitation to the station scale using statistical transformations & ndash; a comparison of methods. *Hydrol. Earth Syst. Sci.* **2012**, *16*, 3383–3390. [CrossRef]
10. Chen, J.; Brissette, F.P.; Chaumont, D.; Braun, M. Finding appropriate bias correction methods in downscaling precipitation for hydrologic impact studies over North America. *Water Resour. Res.* **2013**, *49*, 4187–4205. [CrossRef]
11. Themeßl, M.J.; Gobiet, A.; Leuprecht, A. Empirical-statistical downscaling and error correction of daily precipitation from regional climate models. *Int. J. Climatol.* **2011**, *31*, 1530–1544. [CrossRef]
12. Cannon, A.J.; Sobie, S.R.; Murdock, T.Q. Bias Correction of GCM Precipitation by Quantile Mapping: How Well Do Methods Preserve Changes in Quantiles and Extremes? *J. Clim.* **2015**, *28*, 6938–6959. [CrossRef]
13. Buishand, T.A. Some remarks on the use of daily rainfall models. *J. Hydrol.* **1978**, *36*, 295–308. [CrossRef]
14. Geng, S.; Penning de Vries, F.W.T.; Supit, I. A simple method for generating daily rainfall data. *Agric. For. Meteorol.* **1986**, *36*, 363–376. [CrossRef]
15. Schoof, J.T.; Pryor, S.C.; Surprenant, J. Development of daily precipitation projections for the United States based on probabilistic downscaling. *J. Geophys. Res. Atmos.* **2010**, *115*. [CrossRef]
16. Woolhiser, D.A.; Roldán, J. Stochastic daily precipitation models: 2. A comparison of distributions of amounts. *Water Resour. Res.* **1982**, *18*, 1461–1468. [CrossRef]
17. Burgueño, A.; Martínez, M.D.; Lana, X.; Serra, C. Statistical distributions of the daily rainfall regime in Catalonia (Northeastern Spain) for the years 1950–2000. *Int. J. Climatol.* **2005**, *25*, 1381–1403. [CrossRef]
18. Shin, J.-Y.; Lee, T.; Park, T.; Kim, S. Bias correction of RCM outputs using mixture distributions under multiple extreme weather influences. *Theor. Appl. Climatol.* **2018**. [CrossRef]
19. Papalexiou, S.M.; Koutsoyiannis, D. Entropy based derivation of probability distributions: A case study to daily rainfall. *Adv. Water Resour.* **2012**, *45*, 51–57. [CrossRef]
20. Ye, L.; Hanson, L.S.; Ding, P.; Wang, D.; Vogel, R.M. The probability distribution of daily precipitation at the point and catchment scales in the United States. *Hydrol. Earth Syst. Sci.* **2018**, *22*, 6519–6531. [CrossRef]
21. Howard, T.; Clark, P. Correction and downscaling of NWP wind speed forecasts. *Meteorol. Appl.* **2007**, *14*, 105–116. [CrossRef]

22. Willems, P.; Guillou, A.; Beirlant, J. Bias correction in hydrologic GPD based extreme value analysis by means of a slowly varying function. *J. Hydrol.* **2007**, *338*, 221–236. [CrossRef]
23. Jeon, S.; Paciorek, C.J.; Wehner, M.F. Quantile-based bias correction and uncertainty quantification of extreme event attribution statements. *Weather Clim. Extrem.* **2016**, *12*, 24–32. [CrossRef]
24. Boé, J.; Terray, L.; Habets, F.; Martin, E. Statistical and dynamical downscaling of the Seine basin climate for hydro-meteorological studies. *Int. J. Climatol.* **2007**, *27*, 1643–1655. [CrossRef]
25. Abatzoglou, J.T.; Brown, T.J. A comparison of statistical downscaling methods suited for wildfire applications. *Int. J. Climatol.* **2012**, *32*, 772–780. [CrossRef]
26. Hwang, S.; Graham, W.D. Development and comparative evaluation of a stochastic analog method to downscale daily GCM precipitation. *Hydrol. Earth Syst. Sci.* **2013**, *17*, 4481–4502. [CrossRef]
27. Eum, H.-I.; Simonovic, S.P.; Kim, Y.-O. Climate Change Impact Assessment Using K-Nearest Neighbor Weather Generator: Case Study of the Nakdong River Basin in Korea. *J. Hydrol. Eng.* **2010**, *15*, 772–785. [CrossRef]
28. Seo, S.B.; Kim, Y.-O. Impact of Spatial Aggregation Level of Climate Indicators on a National-Level Selection for Representative Climate Change Scenarios. *Sustainability* **2018**, *10*, 2409. [CrossRef]
29. Eum, H.-I.; Cannon, A.J. Intercomparison of projected changes in climate extremes for South Korea: Application of trend preserving statistical downscaling methods to the CMIP5 ensemble. *Int. J. Climatol.* **2017**, *37*, 3381–3397. [CrossRef]
30. Eagleson, P.S. Dynamics of flood frequency. *Water Resour. Res.* **1972**, *8*, 878–898. [CrossRef]
31. Serinaldi, F. A multisite daily rainfall generator driven by bivariate copula-based mixed distributions. *J. Geophys. Res. Atmos.* **2009**, *114*, D10103. [CrossRef]
32. Kim, D.; Kwon, H.-H.; Lee, S.-O.; Kim, S. Regionalization of the Modified Bartlett–Lewis rectangular pulse stochastic rainfall model across the Korean Peninsula. *J. Hydro Environ. Res.* **2016**, *11*, 123–137. [CrossRef]
33. Sunyer, M.A.; Madsen, H.; Ang, P.H. A comparison of different regional climate models and statistical downscaling methods for extreme rainfall estimation under climate change. *Atmos. Res.* **2012**, *103*, 119–128. [CrossRef]
34. Rodriguez-Iturbe, I.; Cox, D.R.; Isham, V. A point process model for rainfall: Further developments. Proceedings of the Royal Society of London. *Math. Phys. Sci.* **1988**, *417*, 283–298. [CrossRef]
35. Onof, C.; Wheater, H.S. Improvements to the modelling of British rainfall using a modified Random Parameter Bartlett-Lewis Rectangular Pulse Model. *J. Hydrol.* **1994**, *157*, 177–195. [CrossRef]
36. Vrac, M.; Naveau, P. Stochastic downscaling of precipitation: From dry events to heavy rainfalls. *Water Resour. Res.* **2007**, *43*. [CrossRef]
37. Ben-Gai, T.; Bitan, A.; Manes, A.; Alpert, P.; Rubin, S. Spatial and Temporal Changes in Rainfall Frequency Distribution Patterns in Israel. *Theor. Appl. Climatol.* **1998**, *61*, 177–190. [CrossRef]
38. Ines, A.V.M.; Hansen, J.W. Bias correction of daily GCM rainfall for crop simulation studies. *Agric. For. Meteorol.* **2006**, *138*, 44–53. [CrossRef]
39. Piani, C.; Haerter, J.O.; Coppola, E. Statistical bias correction for daily precipitation in regional climate models over Europe. *Theor. Appl. Climatol.* **2010**, *99*, 187–192. [CrossRef]
40. Martins, E.S.; Stedinger, J.R. Generalized maximum-likelihood generalized extreme-value quantile estimators for hydrologic data. *Water Resour. Res.* **2000**, *36*, 737–744. [CrossRef]
41. Katz, R.W.; Parlange, M.B.; Naveau, P. Statistics of extremes in hydrology. *Adv. Water Resour.* **2002**, *25*, 1287–1304. [CrossRef]
42. Nam, W.; Shin, H.; Jung, Y.; Joo, K.; Heo, J.-H. Delineation of the climatic rainfall regions of South Korea based on a multivariate analysis and regional rainfall frequency analyses. *Int. J. Climatol.* **2015**, *35*, 777–793. [CrossRef]
43. Kjeldsen, T.R.; Ahn, H.; Prosdocimi, I.; Heo, J.-H. Mixture Gumbel models for extreme series including infrequent phenomena. *Hydrol. Sci. J.* **2018**, *63*, 1927–1940. [CrossRef]
44. Shin, J.-Y.; Lee, T.; Ouarda, T.B.M.J. Heterogeneous Mixture Distributions for Modeling Multi-source Extreme Rainfalls. *J. Hydrometeorol.* **2015**, *16*, 2639–2657. [CrossRef]
45. Jung, Y.; Shin, J.-Y.; Ahn, H.; Heo, J.-H. The Spatial and Temporal Structure of Extreme Rainfall Trends in South Korea. *Water* **2017**, *9*, 809. [CrossRef]

46. Wallis, J.R.; Schaefer, M.G.; Barker, B.L.; Taylor, G.H. Regional precipitation-frequency analysis and spatial mapping for 24-h and 2-h durations for Washington State. *Hydrol. Earth Syst. Sci.* **2007**, *11*, 415–442. [CrossRef]
47. Parida, B.P. Modelling of Indian summer monsoon rainfall using a four-parameter Kappa distribution. *Int. J. Climatol.* **1999**, *19*, 1389–1398. [CrossRef]
48. Shao, Q.; Wong, H.; Xia, J.; Ip, W.-C. Models for extremes using the extended three-parameter Burr XII system with application to flood frequency analysis/Modèles d'extrêmes utilisant le système Burr XII étendu à trois paramètres et application à l'analyse fréquentielle des crues. *Hydrol. Sci. J.* **2004**, *49*, null-702. [CrossRef]
49. Nadarajah, S.; Bakouch, H.S.; Tahmasbi, R. A generalized Lindley distribution. *Sankhya B* **2011**, *73*, 331–359. [CrossRef]
50. Ganora, D.; Laio, F. Hydrological Applications of the Burr Distribution: Practical Method for Parameter Estimation. *J. Hydrol. Eng.* **2015**, *20*, 04015024. [CrossRef]
51. Norbiato, D.; Borga, M.; Sangati, M.; Zanon, F. Regional frequency analysis of extreme precipitation in the eastern Italian Alps and the August 29, 2003 flash flood. *J. Hydrol.* **2007**, *345*, 149–166. [CrossRef]
52. Park, J.-S.; Jung, H.-S. Modelling Korean extreme rainfall using a Kappa distribution and maximum likelihood estimate. *Theor. Appl. Climatol.* **2002**, *72*, 55–64. [CrossRef]
53. Im, E.-S.; Choi, Y.-W.; Ahn, J.-B. Robust intensification of hydroclimatic intensity over East Asia from multi-model ensemble regional projections. *Theor. Appl. Climatol.* **2017**, *129*, 1241–1254. [CrossRef]
54. Kim, G.; Cha, D.-H.; Park, C.; Lee, G.; Jin, C.-S.; Lee, D.-K.; Suh, M.-S.; Ahn, J.-B.; Min, S.-K.; Hong, S.-Y.; et al. Future changes in extreme precipitation indices over Korea. *Int. J. Climatol.* **2018**, *38*, 862–874. [CrossRef]
55. Giorgi, F.; Jones, C.; Asrar, G.R. Addressing climate information needs at the regional level: The CORDEX framework. *World Meteorol. Organ. Bull.* **2009**, *58*, 175.
56. Oh, S.-G.; Suh, M.-S. Changes in seasonal and diurnal precipitation types during summer over South Korea in the late twenty-first century (2081–2100) projected by the RegCM4.0 based on four RCP scenarios. *Clim. Dyn.* **2018**, *51*, 3041–3060. [CrossRef]
57. Change, I.C. *The Physical Science Basis. Contribution of Working Group I to the Fourth Assessment Report of the Intergovernmental Panel on Climate Change*; IPCC: Geneva, Switzerland, 2007; p. 996.
58. Hanson, C.E.; Palutikof, J.P.; Livermore, M.T.J.; Barring, L.; Bindi, M.; Corte-Real, J.; Durao, R.; Giannakopoulos, C.; Good, P.; Holt, T.; et al. Modelling the impact of climate extremes: An overview of the MICE project. *Clim. Chang.* **2007**, *81*, 163–177. [CrossRef]
59. Giorgi, F.; Gutowski, W.J., Jr. Regional Dynamical Downscaling and the CORDEX Initiative. *Annu. Rev. Environ. Resour.* **2015**, *40*, 467–490. [CrossRef]
60. Mearns, L.O.; Arritt, R.; Biner, S.; Bukovsky, M.S.; McGinnis, S.; Sain, S.; Caya, D.; Correia, J., Jr.; Flory, D.; Gutowski, W.; et al. The North American Regional Climate Change Assessment Program: Overview of Phase I Results. *Bull. Am. Meteorol. Soc.* **2012**, *93*, 1337–1362. [CrossRef]
61. Giorgi, F.; Coppola, E.; Solmon, F.; Mariotti, L.; Sylla, M.B.; Bi, X.; Elguindi, N.; Diro, G.T.; Nair, V.; Giuliani, G.; et al. RegCM4: Model description and preliminary tests over multiple CORDEX domains. *Clim. Res.* **2012**, *52*, 7–29. [CrossRef]
62. Skamarock, W.C.; Klemp, J.B.; Dudhia, J.; Gill, D.O.; Barker, D.M.; Wang, W.; Powers, J.G. *A Description of the Advanced Research WRF Version 2*; National Center for Atmospheric Research Boulder Co Mesoscale and Microscale Div: Boulder, CO, USA, 2005.
63. So, B.-J.; Kim, J.-Y.; Kwon, H.-H.; Lima, C.H.R. Stochastic extreme downscaling model for an assessment of changes in rainfall intensity-duration-frequency curves over South Korea using multiple regional climate models. *J. Hydrol.* **2017**, *553*, 321–337. [CrossRef]
64. Park, C.; Min, S.-K.; Lee, D.; Cha, D.-H.; Suh, M.-S.; Kang, H.-S.; Hong, S.-Y.; Lee, D.-K.; Baek, H.-J.; Boo, K.-O.; et al. Evaluation of multiple regional climate models for summer climate extremes over East Asia. *Clim. Dyn.* **2016**, *46*, 2469–2486. [CrossRef]
65. Kim, S.; Shin, J.-Y.; Ahn, H.; Heo, J.-H. Selecting Climate Models to Determine Future Extreme Rainfall Quantiles. *J. Korean Soc. Hazard Mitig.* **2019**, *19*, 55–69. [CrossRef]
66. Wingo, D.R. Maximum likelihood methods for fitting the burr type XII distribution to multiply (progressively) censored life test data. *Metrika* **1993**, *40*, 203–210. [CrossRef]
67. Hamed, K.; Rao, A.R. *Flood Frequency Analysis*; Taylor & Francis: Milton Park, UK, 2010.
68. Hosking, J.R.M. The four-parameter kappa distribution. *IBM J. Res. Dev.* **1994**, *38*, 251–258. [CrossRef]

69. Vogel, R.M.; Fennessey, N.M. L moment diagrams should replace product moment diagrams. *Water Resour. Res.* **1993**, *29*, 1745–1752. [CrossRef]
70. Kjeldsen, T.R.; Ahn, H.; Prosdocimi, I. On the use of a four-parameter kappa distribution in regional frequency analysis. *Hydrol. Sci. J.* **2017**, *62*, 1354–1363. [CrossRef]
71. Karl, T.R.; Nicholls, N.; Ghazi, A. CLIVAR/GCOS/WMO Workshop on Indices and Indicators for Climate Extremes Workshop Summary. In *Weather and Climate Extremes: Changes, Variations and a Perspective from the Insurance Industry*; Karl, T.R., Nicholls, N., Ghazi, A., Eds.; Springer: Dordrecht, The Netherlands, 1999; pp. 3–7.
72. Kim, K.; Kim, N.W.; Kim, D.P.; Park, S.-S.; Won, Y.S.; Lee, D.; Kim, S.; Heo, J.H.; Choi, Y. *Survey Report of Water Resource Management Method Development in 1999: Drawing Korean Probability Rainfall Map*; Ministry of Construction & Transportation (MOCT): Gwacheon, Korea, 2000.
73. Hosking, J.R.M.; Wallis, J. *Regional Frequency Analysis: An Approach Based on L-Moments*; Cambridge University Press: Cambridge, UK, 2005.
74. Kjeldsen, T.R.; Prosdocimi, I. A bivariate extension of the Hosking and Wallis goodness-of-fit measure for regional distributions. *Water Resour. Res.* **2015**, *51*, 896–907. [CrossRef]
75. Hosking, J.R.M. L-Moments: Analysis and Estimation of Distributions Using Linear Combinations of Order Statistics. *J. R. Stat. Soc. Ser. B* **1990**, *52*, 105–124. [CrossRef]
76. Kay, A.L.; Jones, R.G.; Reynard, N.S. RCM rainfall for UK flood frequency estimation. II. Climate change results. *J. Hydrol.* **2006**, *318*, 163–172. [CrossRef]
77. Blöschl, G.; Hall, J.; Parajka, J.; Perdigão, R.A.P.; Merz, B.; Arheimer, B.; Aronica, G.T.; Bilibashi, A.; Bonacci, O.; Borga, M.; et al. Changing climate shifts timing of European floods. *Science* **2017**, *357*, 588–590. [CrossRef] [PubMed]
78. Dai, A. Increasing drought under global warming in observations and models. *Nat. Clim. Chang.* **2012**, *3*, 52. [CrossRef]
79. Olesen, J.E.; Carter, T.R.; Díaz-Ambrona, C.H.; Fronzek, S.; Heidmann, T.; Hickler, T.; Holt, T.; Minguez, M.I.; Morales, P.; Palutikof, J.P.; et al. Uncertainties in projected impacts of climate change on European agriculture and terrestrial ecosystems based on scenarios from regional climate models. *Clim. Chang.* **2007**, *81*, 123–143. [CrossRef]
80. Kim, K.B.; Bray, M.; Han, D. An improved bias correction scheme based on comparative precipitation characteristics. *Hydrol. Process.* **2015**, *29*, 2258–2266. [CrossRef]
81. Baek, H.-J.; Kim, M.-K.; Kwon, W.-T. Observed short- and long-term changes in summer precipitation over South Korea and their links to large-scale circulation anomalies. *Int. J. Climatol.* **2017**, *37*, 972–986. [CrossRef]
82. Ben Alaya, M.A.; Ouarda, T.B.M.J.; Chebana, F. Non-Gaussian spatiotemporal simulation of multisite daily precipitation: Downscaling framework. *Clim. Dyn.* **2017**. [CrossRef]
83. Costa, V.; Fernandes, W.; Naghettini, M. A Bayesian model for stochastic generation of daily precipitation using an upper-bounded distribution function. *Stoch. Environ. Res. Risk Assess.* **2015**, *29*, 563–576. [CrossRef]
84. Hayes, M.J.; Svoboda, M.D.; Wiihite, D.A.; Vanyarkho, O.V. Monitoring the 1996 Drought Using the Standardized Precipitation Index. *Bull. Am. Meteorol. Soc.* **1999**, *80*, 429–438. [CrossRef]
85. Husak, G.J.; Michaelsen, J.; Funk, C. Use of the gamma distribution to represent monthly rainfall in Africa for drought monitoring applications. *Int. J. Climatol.* **2007**, *27*, 935–944. [CrossRef]
86. Seo, D.-J.; Smith, J.A. Rainfall estimation using raingages and radar—A Bayesian approach: 2. An application. *Stoch. Hydrol. Hydraul.* **1991**, *5*, 31–44. [CrossRef]